

Off-centered vortices in a Bose-Einstein condensate

Tomoya Isoshima,* Jukka Huhtamäki, and Martti M. Salomaa
*Materials Physics Laboratory, Helsinki University of Technology,
 P. O. Box 2200 (Technical Physics), FIN-02015 HUT, Finland*
 (Dated: May 21, 2019)

We study excitations in off-centered vortices in a Bose-Einstein condensate numerically. The displacement of a single vortex and the separation of a doubly quantized vortex are considered. Continual deformations of the core-localized, dipole, and quadrupole excitations accompanying vortex displacement and intervortex separation are observed. The results are interpreted in terms of the precessional motion of the vortices.

PACS numbers: 03.75.Lm, 03.75.Kk, 67.40.Vs

I. INTRODUCTION

Quantized vorticity is a characteristic feature of quantum fluids which accompanies rotational motion. A vortex for complex scalar order parameters is a singular line of rotation which exists inside any closed path with finite velocity circulation. The change of the phase around the vortex line is quantized in units of 2π . In a Bose-Einstein condensate (BEC) of atom gas [1], the first vortex was created by the JILA group [2]. They used a two-component condensate of ^{87}Rb atoms and imprinted a phase winding of 2π onto one component. The position of the vortex core was clearly seen and the precessional motion of the core was observed [2, 3]. In one-component condensate, the ENS group [4] created a vortex state using a rotating trap which consists of an optical spoon and a magnetic trap. Condensates containing up to 4 vortices were observed. Their method can be understood in analogy with fluid motion in a rotating vessel. The idea of a rotating trap has been employed by many groups thereafter.

There is a clear relationship between the rotation frequencies of the trapping potential and the number of vortices. Theoretical and numerical studies have been conducted on vortex formation [5, 6, 7]. Within the Bogoliubov theory, the appearance of a vortex is understood as an excitation of the surface mode [8]. Regarding the escape of a vortex, the excitation level whose wavefunction is localized in the center of the vortex is related to it. In an axisymmetric system in the absence of external rotation, the mode has negative energy. Precessional motion of off-centered vortices in the experiments [2, 3] are also related to this negative amplitude [9]. However, these excitations for a precessing vortex and multiple vortices have not been calculated numerically. Our purpose in this paper is to consider the stabilities of off-centered vortices.

In addition to these singly quantized vortices, vortices with winding numbers 2 and 4 can be formed [10], using a topological method [11]. The image of the cloud of

atoms does not show indications for the splitting of multiply quantized vortices. This stability contradicts with what is widely believed. Therefore, it is urgent to understand the stability of these off-centered vortices and the multiply quantized vortices.

In this paper, we present the condensate wavefunctions for an off-centered vortex, a doubly quantized vortex, and pairs of split vortices. The relation between their excitation spectra and their precessional motion in non-rotating coordinates are clarified.

II. SINGLE OFF-CENTERED VORTEX

We treat a 2-dimensional (xy) system in the rotating frame whose angular velocity is ω . The axis of rotation is perpendicular to the xy plane. Ideally, this represents not only the static condensate in the rotating vessel but also the precessing vortex. The hamiltonian is

$$\hat{H}(\omega) = \hat{H} - \omega \cdot \hat{L} \quad (1)$$

$$\hat{H} = \int \hat{\Psi}^\dagger (-C\nabla^2 + V) \hat{\Psi} + \frac{1}{2}g\hat{\Psi}^\dagger \hat{\Psi}^\dagger \hat{\Psi} \hat{\Psi} d\mathbf{r} \quad (2)$$

$$\hat{L} = \int \hat{\Psi}^\dagger (\mathbf{r} \times \mathbf{p}) \hat{\Psi} d\mathbf{r} \quad (3)$$

where $C = -\hbar^2/(2m)$, $g = 4\pi\hbar^2/m$, and V is the confining potential. We use $\omega = (0, 0, \omega)$ and $\mathbf{r} = (x, y, 0)$. The time-dependent Gross-Pitaevskii equation may be written as

$$\begin{aligned} \{-C\nabla^2 + V(x, y) + g|\phi(x, y, t)|^2 \\ -\omega \cdot \mathbf{r} \times \mathbf{p}\}\phi(x, y, t) = i\hbar \frac{\partial \phi(x, y, t)}{\partial t}. \end{aligned} \quad (4)$$

where $\phi(\mathbf{r})$ is the condensate wavefunction. The time-independent form is

$$\begin{aligned} \{-C\nabla^2 + V(x, y) - \mu + g|\phi(x, y)|^2 \\ -\omega \cdot \mathbf{r} \times \mathbf{p}\}\phi(x, y) = 0. \end{aligned} \quad (5)$$

where μ is the chemical potential. We employ an axisymmetric harmonic trapping potential $V(x, y) = m\omega_{\text{tr}}^2(x^2 + y^2)$ where $\omega_{\text{tr}} = 2\pi \times 200$. The linear number density of particles $N = \int |\phi(\mathbf{r})|^2 d\mathbf{r}$ is fixed to

*Electronic address: tomoya@focus.hut.fi

$1 \times 10^{10} m^{-1}$ in this paper. The mass and the scattering length of particles are $m = 38.17 \times 10^{-27}$ kg and $a = 2.75$ nm, respectively. The angular momentum of the condensate per particle $L = \int \phi^*(\mathbf{r} \times \mathbf{p})\phi d\mathbf{r}/(\hbar N)$ is employed in the following discussion. A condensate with a centered vortex has $L = 1$. Systems with an off-centered vortex have L between 0 and 1. We also use the Thomas-Fermi radius $R_{TF} = 6.79 \mu\text{m}$ as the unit of length.

A. Condensate

It has been pointed out in the literature that the energy of a condensate with a single off-centered vortex does not possess a local minimum within the Thomas-Fermi approximation [12]. In accordance with this, our calculation of the static GP equation Eq. (5) with a single vortex always converges into an axisymmetric vortex or a non-vortex state. To investigate excitations in off-centered vortices we use a condensate wavefunction which satisfies

$$\frac{\max(|\phi(x, y, \Delta t) - \phi(x, y, 0)|)}{\max(|\phi(x, y, 0)|)} < 0.0005 \cdot |\Delta t| \quad (6)$$

where Δt is an imaginary time in the imaginary-time-development method. This condition means that the wavefunction ϕ varies slowly enough in the time scale of the harmonic trap ($0.0005/\nu_{\text{tr}} \ll 1$), as described by on the time-dependent GP Eq. (4). The right-hand side of Eq. (6) is relaxed to $0.03 \cdot |\Delta t|$ for $L < 0.2$.

For various initial displacements δr , we obtain a set of $\phi(x, y)$ and ω which satisfy Eq. (6). The angular velocities ω that have been determined in this way are discussed in Sec. IV. Figure 1(a) shows the density profiles for condensate ϕ with an off-centered vortex. The relation between the angular momentum and the displacement of a vortex core is plotted in Fig. 1(b). Figure 1(c) displays a normalized energy of the condensate

$$\Delta E' = (E - E_0)/(E_1 - E_0) \quad (7)$$

where E_0 , E_1 , and E are the energy of condensate without vortex, with a centered vortex, and with an off-centered vortex, respectively.

B. Excitation Spectrum

Excitations from a BEC have been described in the framework of the Bogoliubov equations in Ref. [17]. They play a significant role in determining the vortex stability. Nevertheless, these modes in off-centered vortices have not been analyzed so far. An excitation whose energy is ε consists of two wavefunctions, u and v , each with different momenta. They are determined as the solutions to the eigensystem of Bogoliubov equations [1]

$$(-C\nabla^2 + V - \mu + 2g|\phi|^2 - \boldsymbol{\omega} \cdot \mathbf{r} \times \mathbf{p}) u$$

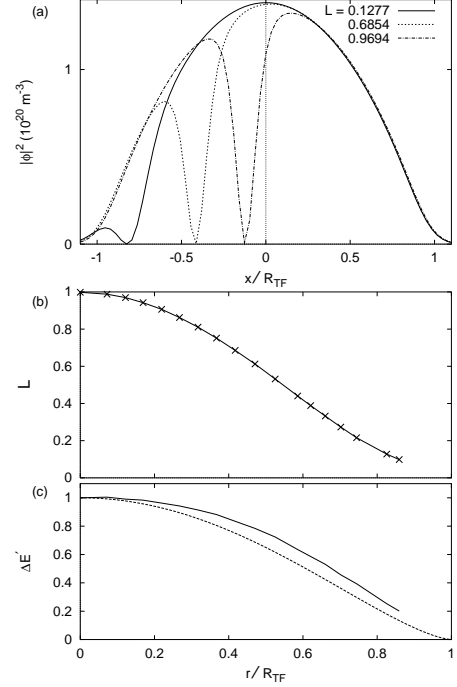


FIG. 1: (a) Density of the condensate along the x -axis. The angular momenta L are 0.1277, 0.6854, and 0.9694, respectively. (b) Displacement of vortex core vs. angular momentum of the condensate per particle. The displacement vanishes for $L = 1$. (c) Displacement of the vortex core r vs the relative energy of condensate $\Delta E'$. The solid line represents the numerical results. The dotted line is obtained fitting $(1 - (r/R_{TF})^2)^{3/2}$, taken from Eq. (49) in Ref. [12].

$$\begin{aligned} -g\phi^2 v &= \varepsilon u \quad (8) \\ -(-C\nabla^2 + V - \mu + 2g|\phi|^2 + \boldsymbol{\omega} \cdot \mathbf{r} \times \mathbf{p}) v \\ + g\phi^{*2} u &= \varepsilon v. \quad (9) \end{aligned}$$

The modes with negative $\int (|u|^2 - |v|^2) d\mathbf{r}$ are ignored. Two of the lowest excitations are the condensate mode (with $\varepsilon = 0$, $u = \phi$, $v = \phi^*$) and the core-localized mode. We ignore the mode with the smallest $|\varepsilon|$ as the condensate mode.

The wavefunctions u and v are obtained through the Bogoliubov equations Eqs. (8) and (9). We denote their angular momenta using

$$\mathcal{A}(u) \equiv \frac{\int u^*(\mathbf{r} \times \mathbf{p})u d\mathbf{r}}{\hbar \int |u|^2 d\mathbf{r}}, \quad (10)$$

$$q_\theta \equiv \frac{\mathcal{A}(u) \int |u|^2 d\mathbf{r} + \mathcal{A}(v) \int |v|^2 d\mathbf{r} - L}{\int (|u|^2 + |v|^2) d\mathbf{r}}, \quad (11)$$

where q_θ reduces to an integer for axisymmetric systems [13]. Since ω varies for various values of the angular momentum of the condensate, we use the approximate energy levels in the laboratory frame

$$\varepsilon_{\text{lab}} \equiv \varepsilon + \omega q_\theta. \quad (12)$$

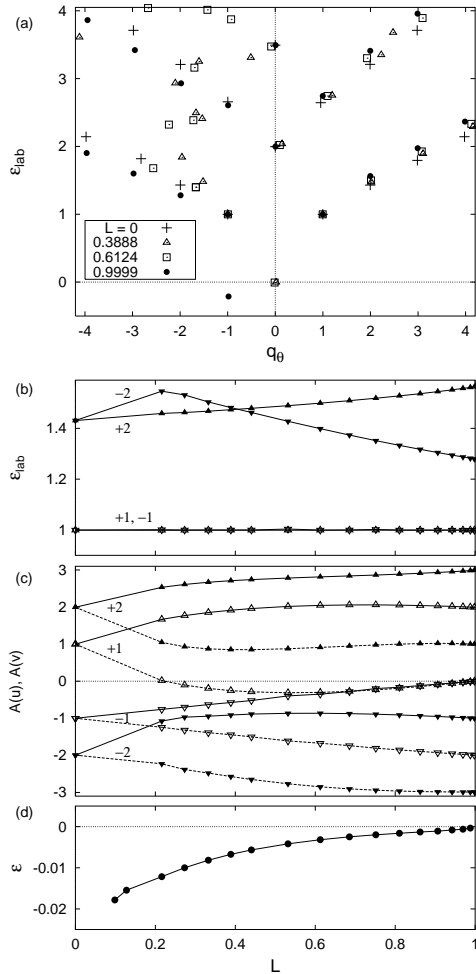


FIG. 2: (a) Excitation spectra of a Bose-Einstein condensate with a centered vortex, an off-centered vortex, and without a vortex. The vertical scale measures is the excitation energy, ε_{lab} . The horizontal axis indicates the angular momentum q_θ . The cross, triangle, square, and the bullet correspond to the angular momenta of the condensate with $L = 0, 0.38, 0.61$, and 1 , respectively. (b) Excitation energies of the dipole modes (labelled $+1$ and -1) and the quadrupole modes $(+2, -2)$. (c) The angular momenta of the wavefunctions u (solid line) and v (dotted line) for the dipole $(+1, -1)$ and quadrupole modes $(+2, -2)$. (d) Energy ε of the lowest core excitation in the rotating frame is negative and it satisfies $|\varepsilon| \ll 1$. This is in accordance with the weak instability of the GP equation, Eq. (6).

The excitation energies are normalized by the trap unit $\hbar\omega_{\text{tr}}$ from now on. Figure 2(a) displays the computed excitation energies, ε , and the corresponding angular momenta, q_θ . Some of the modes, for example those with $(\varepsilon, q_\theta) = (2, 0), (1, \pm 1)$ are robust. Some of the core-localized modes have $(\varepsilon_{\text{lab}}, q_\theta) = (0, 0)$. These are discussed in Sec. II C. The modes with $(\varepsilon_{\text{lab}}, q_\theta) \simeq (1, \pm 1), (1.5, \pm 2)$ are discussed in Sec. II D.

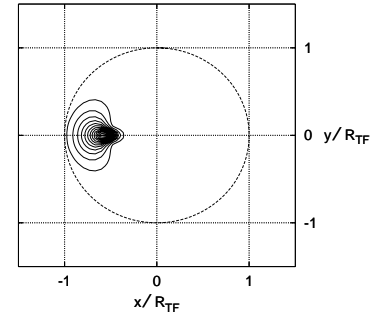


FIG. 3: Wavefunction $|u|^2$ of the core-localized mode. Solid lines denote contours of density. There occurs a peak density in the vortex core. The dotted line shows R_{TF} .

C. Core-Localized Mode

There always occurs an excitation whose energy is just slightly below zero ($-0.01 < \varepsilon < 0$) in the rotating frame [see Figs. 2(a) and 2(d)]. When $L = 1$, the vortex is in the center of a system and the wavefunction u of this excitation do not possess an angular momentum (thus $q_\theta = -1$). It has a sharp peak in the vortex core. These results are equivalent with those for axisymmetric calculations [13].

Once the vortex becomes off-centered, both wavefunctions u and v localize in the vortex core as shown in Fig. 3. Each of them features a sharp peak in the vortex core and its foot extends towards the surface of the condensate. The angular momenta of u and v have opposite signs but similar amplitudes. The negative energy and the localization at the core means that this mode is parallel with the core localized mode in the axisymmetric calculations [13, 14].

The angular momenta of u of the core-localized mode varies between 1 to 4 . The corresponding wavefunctions v have opposite angular momenta. Their average q_θ almost vanishes ($|q_\theta| \ll 1$); the points at $(0,0)$ in Fig. 2(a) mean this. This behavior of the core-localized modes is unexpected. One possible underlying cause may be that condensate wavefunctions of off-centered vortices are not fully stable [Eq. (6)] solutions of the GP equation.

D. Dipole and Quadrupole Modes

Excitations having the lowest positive energy at $q_\theta = \pm 1$ and $\simeq \pm 2$ are classified as dipole and quadrupole modes. Figure 2(b) shows the energy for these modes. The energies of the dipole modes equal almost 1 trap unit ($\hbar\omega_{\text{tr}}$). The dipole modes are known as responsible for the center-of-mass motion [15]. Therefore, they are not affected by various profiles inside the condensate. The angular momenta $\mathcal{A}(u)$ and $\mathcal{A}(v)$ are plotted in Fig. 2(c).

These excitations show continual transformation along with variation of the vortex displacement.

The condensate in a 2-dimensional harmonic potential has two quadrupole modes. A splitting between the quadrupole frequencies $\varepsilon_{\text{lab}}(+2) - \varepsilon_{\text{lab}}(-2)$ is inverted at $L \simeq 0.4$, while it is proportional to L in systems with a centered vortex [15]. The corresponding eigen oscillation of condensate, called the scissors mode has been observed experimentally [16] to evaluate an angular momentum of a condensate.

For $\omega \gtrsim 0.35\omega_{\text{tr}}$, the excitation energies of the modes with $q_\theta > 2$ approach close each other, and their wavefunctions become entangled. The angular momenta of excitations in this region ($L < 0.2$) are omitted in Figs. 2 for the sake of clarity.

III. TWO VORTICES

A vortex with the winding number 2 has been formed in a condensate of Na atoms [10]. It is believed that such vortices spontaneously split into two singly quantized vortices, while the experimental data does not indicate any signs of the splitting. In this section, we investigate the excitation spectra of systems with two vortices to inspect their stability in the splitting process.

Each of the GP calculations starts from an initial wavefunction with two slightly displaced vortices under a fixed angular velocity, Ω . The resulting angular momenta are controlled through this ω . The GP equation has a static solution for about $60 < \omega/(2\pi) < 110$. The corresponding range of angular momenta is from 1.2 to 1.8. Many vortices enter into the condensate for higher $\omega/(2\pi) > 110$ and the vortices disappear for $\omega/(2\pi) < 60$. Figure 4 shows the density profiles of the condensate for various angular momenta.

Using the condensate wavefunctions, the excitations from it are calculated with the Bogoliubov equations, Eqs. (8) and (9). Figure 5(a) shows that the modes with positive energy are robust against the separation of the vortices. The lowest positive-energy modes, with $q_\theta \simeq \pm 1$ and $q_\theta \simeq \pm 2$, are classified as dipole and quadrupole modes. Their computed angular momenta and energies in the laboratory frame are presented in Fig. 5(b) and 5(c).

Contrastingly, the modes with $\varepsilon_{\text{lab}} < 0$ show various energies in Fig. 5(a). This behavior is caused by difficulties in calculating the angular momenta through Eq. (11). Figure 5(d) shows the energy levels of two excitations with the lowest real part in the rotating frame. For $1.2 < L < 1.57$, there occur two conjugate pairs of complex eigenvalues, both of them has a large imaginary part. For larger L , one of them has a large imaginary part. Figure 6 displays the wavefunctions of these lowest modes. One of them has an imaginary eigenvalue, while the other one has a real eigenvalue. Both of them display a peak in the vortex core.

A doubly quantized vortex in a two-dimensional sys-

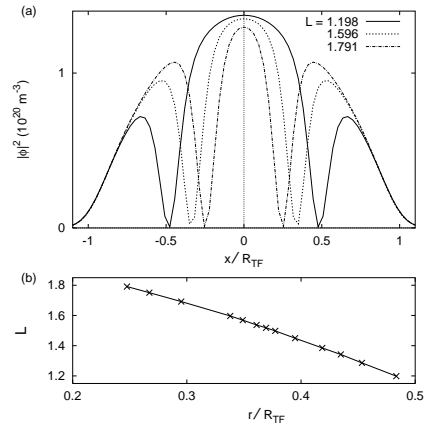


FIG. 4: (a) Density of condensate along x -axis. A condensate has two vortices and both of them are in x -axis. Angular momenta L are 1.198, 1.596, and 1.791 respectively. (b) Displacement of vortex core vs angular momentum of the condensate per particle. The displacement will be zero when the angular momentum of the condensate is 2.

tem has two negative excitations, those for $q_\theta = -1$ and -2 . One of them with $q_\theta = -2$ sometimes has a complex energy, depending on the particle density in the system, see Ref. [18]. This feature is equivalent to those of our results depicted in Fig. 5(d) for higher L . The pairs of complex modes for lower L in Fig. 5(d) may be understood as an entanglement of the complex core-localized modes for each of the singly quantized vortices discussed in Sec. II C.

IV. PRECESSION FREQUENCIES

The above results are calculated in the rotating frame. It is not self-evident whether they may be interpreted as results for precessing vortices in the laboratory frame. To estimate the validity of condensate wavefunction, we carry out time-dependent Gross-Pitaevskii (GP) calculations in the laboratory frame. The above results of the static GP equation are allowed to develop in time according to Eq. (4).

The condensate shows precessional motion of the vortices for both the single-vortex and the two-vortex cases. Figure 7 shows the precessional angular velocity, ω_{pr} . The rotation frequency ω that we obtained in the static calculations in the Sec. II and III are also plotted. The two frequencies agree well. It means that our results in the rotating frame can also be recognized as those in the laboratory frame. The excitation modes, including the core mode, precess following the vortex core there.

The relation between the lowest excitation energy and the precessional frequencies is partially verified. The lowest energy satisfies $|\varepsilon| \ll 1$ in the static calculations. However, the corresponding energies ε_{lab} are not reliable

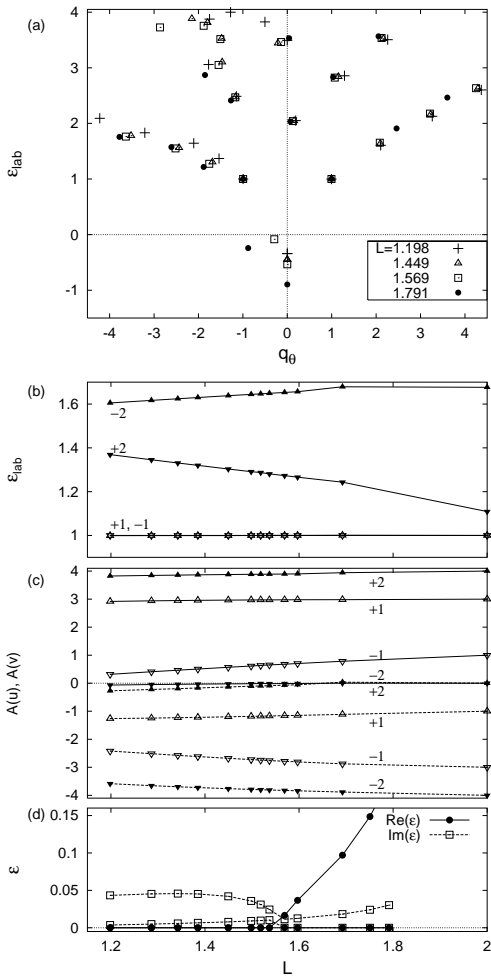


FIG. 5: (a) Excitation spectra of a Bose-Einstein condensate with a pair of off-centered vortices. The vertical axis denotes the excitation energy, ε_{lab} . Some of the modes plotted for $\varepsilon_{\text{lab}} < 0$ have complex energies. Their real parts are plotted. The horizontal axis is the angular momentum, q_θ . The cross, triangle, square, and bullet correspond to the angular momenta of condensate 1.198, 1.449, 1.569, and 1.791, respectively. (b) Energy levels ε_{lab} of the quadrupole and dipole modes in the laboratory frame. (c) Angular momenta of the quadrupole and dipole modes. Solid lines show those of u , while the dashed lines correspond to v . (d) Two excitations with the lowest $\text{Re}(\varepsilon)$. Conjugate modes with negative imaginary parts are not plotted. A system has two conjugate pairs of complex eigenvalues or one pair of complex eigenvalues and one real eigenvalue. The real and imaginary parts are plotted independently. The points at $L = 2$ in (a) and (b) are taken from axisymmetric calculations.

since the angular momenta q_θ of the core modes are close to zero and they are not smoothly connected to the values in the axisymmetric system.

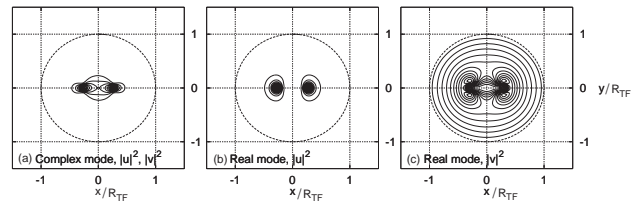


FIG. 6: (a) Wavefunction $|u|^2$ of a complex mode; the wavefunction v of the complex mode is the conjugate of u . The energy levels of these modes are $\pm 0.0241i$. (b) (c) Wavefunctions $|u|^2$ and $|v|^2$ of the lowest mode. The dotted line shows R_{TF} . The energy eigenvalue of this mode is $\varepsilon_{\text{lab}} = -0.2329$. The angular momenta of condensate is 1.750.

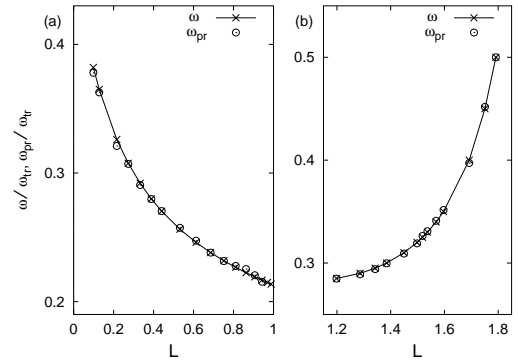


FIG. 7: Circles represent the precessional angular velocities according to time-dependent calculations; lines show the angular velocity $\omega/\omega_{\text{tr}}$ that gives each value of angular momentum L . The vertical axis is normalized by the trap frequency. (a) For systems with a vortex. (b) For systems with two vortices.

V. DISCUSSION

The excitation spectra of Bose Einstein condensate with off centered vortices have been investigated. The dipole and quadrupole modes deform continuously for various values of angular momentum from singly and doubly quantized axisymmetric vortex states towards the non-vortex state. The relation between the angular momenta of the condensate and the separation of the quadrupole excitation energies are shown in the non-axisymmetric vortex states with 1 and 2 vortices.

It is confirmed that a core-localized mode exists for each off-centered vortex in the rotating frame. The rotation frequencies fit well with the precession frequencies of vortices in the laboratory frame. The core-localized mode also precesses following the vortex core in system with one and two vortices.

On splitting of the doubly quantized vortex, the existence of two core localized excitations is confirmed throughout the calculated range of the L . The lowest value of their real part for the energy is zero

($\min[\text{Re}(\varepsilon)] \ll 1$) in the rotating frame. And the rotating velocities ω are equal to the precessing velocities ω_{pr} that are numerically obtained [Fig. 7(b)]. In analogy with the core mode of a single-vortex system the modes are supposed to be responsible for the precessional motion of the vortex.

The surface excitation modes which are related to the nucleation of vortices are not discussed in this paper. This is because their wavefunctions entangle with each other at higher rotation frequencies. We think that a similar entanglement is affecting the core-localized modes.

Non-axisymmetric confining traps are not treated in this paper. For understanding the vortex-nucleation process [5, 6, 19], research on the surface modes in a nonaxisymmetric confining trap should be carried out.

Acknowledgements

Authors thank CSC-Scientific Computing Ltd (Finland) for computer resources. We are grateful to M. Nakahara, T. P. Simula, and S. M. M. Virtanen for stimulating discussions. One of the authors (TI) is supported by the bilateral exchange programme between the Academy of Finland and the Japan Society for the Promotion of Science.

[1] C. J. Pethick and H. Smith, *Bose-Einstein Condensation in Dilute Gases* (Cambridge University Press, Cambridge, England, 2002).

[2] M. R. Matthews, B. P. Anderson, P. C. Haljan, D. S. Hall, C. E. Wieman, and E. A. Cornell, Phys. Rev. Lett. **83**, 2498 (1999).

[3] B. P. Anderson, P. C. Haljan, C. E. Wieman, and E. A. Cornell, Phys. Rev. Lett. **85**, 2857 (2000).

[4] K. W. Madison, F. Chevy, W. Wohlleben, and J. Dalibard, Phys. Rev. Lett. **84**, 806 (2000).

[5] K. W. Madison, F. Chevy, V. Bretin, and J. Dalibard, Phys. Rev. Lett. **86**, 4443 (2001).

[6] M. Tsubota, K. Kasamatsu, and M. Ueda, Phys. Rev. A **65**, 023603 (2002).

[7] J. R. Anglin, Phys. Rev. A **65**, 063611 (2002).

[8] F. Dalfovo, S. Giorgini, M. Giuseppi, L. Pitaevskii, and S. Stringari, Phys. Rev. A **56**, 3840 (1997).

[9] D. L. Feder, A. A. Svidzinsky, A. L. Fetter, and C. W. Clark, Phys. Rev. Lett. **86**, 564 (2001).

[10] A. E. Leanhardt, A. Görlitz, A. P. Chikkatur, D. Kielpinski, Y. Shin, D. E. Pritchard, and W. Ketterle, Phys. Rev. Lett. **89**, 190403 (2002).

[11] M. Nakahara, T. Isoshima, K. Machida, S.-i. Ogawa, and T. Ohmi, Physica B **284**, 17 (2000); T. Isoshima, M. Nakahara, T. Ohmi, and K. Machida, Phys. Rev. A **61**, 063610 (2000); S.-i. Ogawa, M. Möttönen, M. Nakahara, T. Ohmi, and H. Shimada, Phys. Rev. A **66**, 013617 (2002); M. Möttönen, N. Matsumoto, M. Nakahara, and T. Ohmi, e-print cond-mat/0205542, to be published in J. Phys.: Cond. Matt.

[12] A. L. Fetter and A. A. Svidzinsky, e-print cond-mat/0102003.

[13] T. Isoshima, K. Machida, Phys. Rev. A **59**, 2203 (1999); T. Isoshima, K. Machida, Phys. Rev. A **60**, 3313 (1999).

[14] S. M. M. Virtanen, T. P. Simula, and M. M. Salomaa, Phys. Rev. Lett. **86**, 2704 (2001).

[15] F. Zambelli and S. Stringari, Phys. Rev. Lett. **81**, 1754 (1998).

[16] F. Chevy, K. W. Madison, and J. Dalibard, Phys. Rev. Lett. **85**, 2223 (2000).

[17] J. M. Vogels, K. Xu, C. Raman, J. R. Abo-Shaeer, and W. Ketterle, Phys. Rev. Lett. **88**, 060402 (2002).

[18] H. Pu, C. K. Law, J. H. Eberly, and N. P. Bigelow, Phys. Rev. A **59**, 1533 (1999).

[19] E. Lundh, J.-P. Martikainen, and K.-A. Suominen, e-print cond-mat/0211401.